Surface Review and Letters, Vol. 30, No. 8 (2023) 2350056 (14 pages)

DOI: 10.1142/S0218625X23500567

World Scientific
www.worldscientific.com

EXPERIMENTAL INVESTIGATION AND OPTIMIZATION OF MACHINING PARAMETERS IN WEDM OF ZrO_2 AND SEASHELL POWDER-REINFORCED BIODEGRADABLE AZ31 Mg ALLOY COMPOSITE

V. SESHADHRI[*,‡], R. SARALA[*,§], S. V. ALAGARSAMY[†,¶] and C. ILAIYA PERUMAL[*,‖]

[*]*Department of Mechanical Engineering, Alagappa Chettiar Government College of Engineering and Technology, Karaikudi 630 004, Tamil Nadu, India*

[†]*Department of Mechanical Engineering, Mahath Amma Institute of Engineering and Technology, Pudukkottai 622 101, Tamil Nadu, India*

[‡]*seshadhiri2009@gmail.com*
[§]*sarala.sutharson@gmail.com*
[¶]*s.alagarsamy88@gmail.com*
[‖]*ipdesign2012@gmail.com*

Received 1 December 2022
Revised 16 April 2023
Accepted 7 May 2023
Published 21 June 2023

In the current scenario, many researchers aspire to develop biodegradable material for biomedical implant applications. Magnesium (Mg)-based alloys are most promising materials since they have mechanical properties similar to human bone. In this study, Mg alloy AZ31 matrix was reinforced with a seashell powder (2 wt.%) and zirconium dioxide (10 wt.%) using bottom pouring stir casting furnace. Scanning electron microscope (SEM) with energy dispersive spectroscopy (EDS) images confirms the proper distribution of reinforcement throughout the matrix. This study analyzed the influence of WEDM process parameters for the material removal rate (MRR) and surface roughness (SR) of the proposed composite. According to Taguchi's L_9 (3^3) orthogonal array the machining was performed to investigate the ideal machining parameters with a range of pulse current (I_p) 6–8 amps, pulse-on time (T_{on}) 5–15 μs and pulse-off time (T_{off}) 10–30 μs, respectively. Analysis of variance (ANOVA) result confirms that I_p (45.86%) has the most influencing parameter affecting the MRR and SR, followed by T_{on} (25.10%) and T_{off} (17.19%), respectively. Furthermore, Technique for Order Preference by Similar Ideal Solution (TOPSIS) and desirability approach was employed to find the optimal parameter combinations to attain the best combined output responses.

Keywords: AZ31 Mg alloy; ANOVA; seashell; stir casting; TOPSIS; WEDM; ZrO_2.

‡Corresponding author.

1. Introduction

In the past decades, metal implants have played a major role in orthopedics. They require strong resistance to corrosion if implanted inside the human body. Steel and titanium are the major materials contributed for the bone implants.[1,3] Since the metallic implant is a new substance to the human body, it may develop long-term adverse effects, higher risk of local inflammation and leads to the second surgery.[4,5] To overcome these complications Magnesium-based biodegradable implants have been suggested which makes it as a desirable metal for the human body. The density of Magnesium (1.738 g/cm^3) and human bone (1.5–2.0 g/cm^3) is very similar which attracts many researchers to use Magnesium as bone imparts.[6] On contrary, the corrosion rate of Magnesium is too high, so the Magnesium-based implant degrades quickly before bone healing or regeneration. To improve the strength and corrosion resistance of Mg alloy, hard or soft ceramic particulates were reinforced. In general, the machining of reinforced composites is more complicated in traditional machining due to the enhancement of properties like strength, hardness and stiffness. Hence, non-traditional machining such as EDM, WEDM is preferred.[7] Many researchers studied about the fabrication of Magnesium-based Metal Matrix Composites (MMC) and machinability using WEDM process. ANOVA results by Razak *et al.* revealed that spark on time is the most influencing parameter affecting the SR while machining the AZ31 magnesium alloy.[8] Vijayabhaskar *et al.*[9] described that the optimization of WEDM machining parameter such as voltage, T_{on}, T_{off}, wire feed rate and wt.% nano-SiC particles of nano-SiC-reinforced Magnesium matrix composites were studied using Response Surface Methodology (RSM). They also stated that voltage was the chief imperative factor for improving both MRR and SR. Randeep Singh Gill *et al.*[10] developed Mg-4Zn alloy using resistance heating furnace and Taguchi's L_9 orthogonal design has been used to find the optimum process parameter of the WEDM process for the response such as SR and MRR. Karthik *et al.*[11] explored the effect of WEDM parameters on SR for AZ31B Mg alloy using molybdenum wire and they reported that T_{on} was the more noteworthy factor on SR. Muniappan *et al.*[12] optimized the WEDM process of AZ91 Mg alloy using multi objective optimization by ratio analysis and revealed the optimal conditions of parameters for obtaining the highest cutting rate and lesser kerf width. Kavimani *et al.*[13] stated the influence of machining factors on MRR and SR during the WEDM process of Mg-SiC-Graphene composite using Copper wire as an electrode. They observed that MRR increases with increase in pulse-on time and also MRR decreases when there is an increase in reinforcement content. Meanwhile, the SR increases with increase in reinforcement content and pulse-on time. Based on the earlier studies, it could be concluded that study on WEDM of Magnesium MMCs was limited when compared to other materials, namely Aluminium and titanium-based MMCs. By considering this view point, the aim of this work is to fabricate the composite of AZ31 Magnesium alloy reinforced with ZrO_2 and seashell powder by bottom pouring stir casting method. These developed composites are machined by WEDM process and also the input parameters are taken as I_p, T_{on} and T_{off}. The optimized machining parameters for obtaining the maximum MRR with minimum SR are identified by Taguchi coupled TOPSIS and desirability approach.

2. Materials and Methods

In this research work, AZ31 Mg alloy was taken as matrix element, ZrO_2 and seashell powders were utilized as reinforcements because of its high strength. Pure Magnesium reacts with environment leading to rapid corrosion. Addition of Aluminum and zinc helps to diminish the corrosion rate of the Mg alloy.[4] The mixture of ZrO_2 and seashell powder offers more resistance to corrosion and also improves grain refinement thus enhancing the mechanical properties.[14] Initially, the collected seashells were boiled in water to remove sea salt and organic matter. Again, they were rinsed with distilled water 3–4 times and then dried by oven. In order to obtain the uniform particle size of seashell, they were ball-milled for 2 h. The ZrO_2 particles having an average particle size of 10 μm were purchased from Prichem, Coimbatore. In this study, the AZ31 Mg alloy was reinforced with 10 wt.% of ZrO_2 and 2 wt.% of ball-milled seashell powder for enhancing the wear and corrosion resistance. Many researchers fabricate the Magnesium matrix composite by a powder metallurgy process,

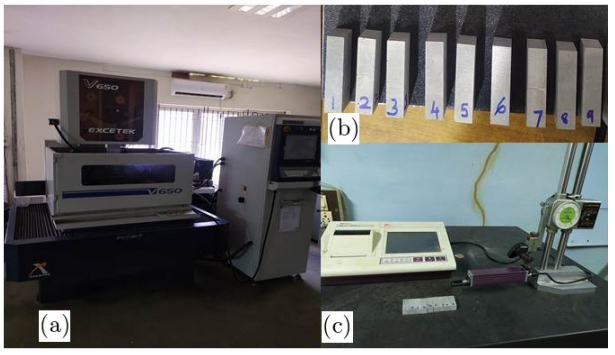

Fig. 1. (a) WEDM setup, (b) machined composite and (c) Mitutoyo Talysurf SJ-310 (surface roughness tester).

but it is very expensive as compared with other methods (casting).[15] The casting of Magnesium is quite complicated in normal atmospheric condition, it requires varied controlled environment. Hence, the composites were fabricated by using bottom pouring stir casting with argon gas controlled furnace. The presence and proper distribution of reinforcements were analyzed through SEM and EDS analysis.

The machinability studies for the developed composites were analyzed by WEDM process. The machining was carried out using CNC WEDM make EXCETEC (Taiwan) model 650 V (Fig. 1(a)) in CIPET located at Madurai, Tamil Nadu, India. The general parameters for WEDM are provided in Table 1. WEDM usually consists of a machine tool, a power supply unit and flushing unit. De-mineralized water is used as a dielectric fluid and also acts as a cooling medium. Initially, the work piece was submerged under the de-mineralized water for reducing the heat generation as well as breakage of wire electrode. Due to its excellent tensile strength, electrical conductivity and low cost, a brass wire of 0.25 mm diameter was used as wire electrode. The fabricated composite specimen in the size of 140 mm × 100 mm × 10 mm was selected for machining. Based on the earlier studies,[16,17] three machining parameters were chosen as input parameters such as I_p, T_{on} and T_{off}, respectively. Table 2 depicts the input parameters and their levels. The output responses were considered as MRR and SR. The experimental work has been carried out as per Taguchi's L_9 orthogonal layout as shown in Table 3. After machining each sample was numbered (Fig. 1(b)) and weights of each specimen were measured using the physical weighing machine. MRR is calculated by determining the amount of material removed with respect to the time taken for machining the specimen. To estimate the MRR, the following equation is used.

$$\text{MRR} = \frac{W_{\text{bm}} - W_{\text{am}}}{T}, \tag{1}$$

where W_{bm} and W_{am} are weight of the specimen before and after machining (g), and T is machining time (min). The surface roughness tester (Mitutoyo Talysurf SJ-310) is shown in Fig. 1(c) and it was used to assess the SR value. The average value of SR was taken into consideration after SR of the machined specimens was determined at three separate points on each machined surface.

Table 1. General parameters of WEDM machine.

Parameters	Range/values
Dielectric Fluid	De-ionized water
Wire material	Brass
Servo voltage	36 V
Gap Voltage	36 V
Wire Diameter	0.25 mm
Wire feed rate	2 m/min
Wire Tension	10 N
Frequency	100 Hz

Table 2. Machining parameters and levels.

Machining parameter	Unit	Level 1	Level 2	Level 3
Pulse current (I_p)	amps	6	8	10
Pulse-on time (T_{on})	μs	5	10	15
Pulse-off time (T_{off})	μs	10	20	30

Table 3. L_9 Orthogonal array with output response.

Ex. No.	I_p (amps)	T_{on} (μs)	T_{off} (μs)	MRR (g/min)	SR (μm)
1	6	5	10	0.25925	3.46
2	6	10	20	0.36665	4.16
3	6	15	30	0.39493	4.24
4	8	5	20	0.24470	3.83
5	8	10	30	0.35503	4.50
6	8	15	10	0.38661	4.75
7	10	5	30	0.24405	3.50
8	10	10	10	0.30599	5.19
9	10	15	20	0.36740	4.92

3. Methodologies and Implementations

3.1. *Taguchi method*

In this analysis, signal-to-noise ratio (S/N) was taken into consideration which helped in finding out the optimum condition of the machining parameter for the selected responses.[18] Basically, three types of constraints were used to estimate the S/N ratio. They are "larger the better", "nominal the better", and "smaller the better".[19] During this investigation, MRR and SR are the two output responses to predict the optimal conditions. Here, the MRR of larger amount of metal has to be removed with respect to time, so larger the better is suggested. Similarly, SR of the machined surface should be low, so smaller the better is used to find the optimized machining parameter. In computing the S/N ratio of the responses, the following equations are used.[20]

$$S/N \text{ ratio} = -10\log_{10}(1/n)\sum_{k=1}^{n}\frac{1}{Y_{ij}^2}, \tag{2}$$

$$S/N \text{ ratio} = -10\log_{10}(1/n)\sum_{k=1}^{n}Y_{ij}^2, \tag{3}$$

where n is the number of factors, Y_{ij} is the output, $i = 1, 2, 3, \ldots, n$, and $j = 1, 2, 3, \ldots, k$. Table 4 depicts the calculated S/N ratios for the output responses.

3.2. *TOPSIS approach*

Technique for order preference by similar ideal solution (TOPSIS) approach is a multi-objective optimization method used to find the best optimized parameter.[21–23] This approach was originally invented by Hwang and Yoon in 1981.[24] It has been employed to highlight the finest alternatives that are closest to both the positive ideal solution and the opposite of that solution.[25–27] Here, the machining parameters are optimized for the multi-response like MRR and SR. The optimum machining parameters are obtained in the means of performance scores. The following steps are used to find the optimum solution.

Step 1: Determining the normalized values from the output responses. The normalized matrix $\overline{X}_{ij}$ was calculated using the following equation:

$$\bar{X}_{ij} = \frac{X_{ij}}{\sqrt{\sum_{i=1}^{m} X_{ij}^2}} \qquad i = 1, 2, \ldots, m, \quad j = 1, 2, \ldots, n, \tag{4}$$

where I is the number of experimental runs, j is the number of responses and X_{ij} is the experimental value of ith term affiliated with jth response.

Step 2: The weighted normalized decision matrix values are computed by the product of normalized variables with weighted variations on $\sum_{j=1}^{n} W_j = 0.5$. The weighted normalized number variable (V_{ij}) is obtained using the following equation:

$$V_{ij} = \bar{X}_{ij} \times W_j \quad i = 1, 2, \ldots, m, j = 1, 2, \ldots, n. \tag{5}$$

Table 5 shows the calculated normalized matrix and the weighted normalized matrix.

Step 3: Finding the ideal alternate to the best performance (V^+) and worst performance (V^-) measures for all output response using the following equations:

$$V^+ = \{(\max V_{ij} | j \in C_c), (\min V_{ij} | j \in C_c)\} = \{V_{ij}^- | j = 1, 2, \ldots, m\}, \tag{6}$$

Table 4. Output responses and their S/N ratios.

	Output responses		S/N ratios	
Ex. No.	MRR (g/min)	SR (μm)	MRR (dB)	SR (dB)
1	0.25925	3.46	−11.7256	−10.7815
2	0.36665	4.16	−8.7150	−12.3819
3	0.39493	4.24	−8.0696	−12.5473
4	0.24470	3.83	−12.2273	−11.664
5	0.35503	4.50	−8.9947	−13.0643
6	0.38661	4.75	−8.2545	−13.5339
7	0.24405	3.50	−12.2504	−10.8814
8	0.30599	5.19	−10.2859	−14.3033
9	0.36740	4.92	−8.6972	−13.8393

Table 5. Normalized and weighted normalized value.

	Normalized value		Weighed normalized value	
Ex. No.	MRR	SR	MRR	SR
1	0.25925	3.468	0.26172	0.26734
2	0.36665	4.160	0.37015	0.32069
3	0.39493	4.242	0.39870	0.32701
4	0.24470	3.833	0.24703	0.29548
5	0.35503	4.501	0.35841	0.34690
6	0.38661	4.751	0.39030	0.36625
7	0.24405	3.502	0.24638	0.26981
8	0.30599	5.194	0.30891	0.40040
9	0.36740	4.920	0.37090	0.37928

$$V^- = \{(\min V_{ij}|j \in C_c), (\max V_{ij}|j \in C_c)\} = \{V_{ij}^-|j = 1, 2, \ldots, m\}, \quad (7)$$

where V^+ indicates the best ideal result {0.19935, 0.13367} and V^- indicates the worst ideal result {0.12319, 0.2002}.

Step 4: Evaluating the execution of the responses, namely superior alternate distance (S_i^+) from the V^+ result and inferior alternate (S_i^-) from the V^- result. S_i^+ and S_i^- values were determined by using the following equations:

$$S_i^+ = \sqrt{\sum_{j=1}^{m} (V_{ij} - V^+)^2}, \quad (8)$$

$$S_i^- = \sqrt{\sum_{j=1}^{m} (V_{ij} - V^-)^2}. \quad (9)$$

Step 5: The final step of the method has determined the performance score (P_i) from S_i^+ and S_i^- by using the following equation:

$$P_i = \frac{S_i^-}{S_i^+ + S_i^-}. \quad (10)$$

Table 6 depicts the inferior alternatives with performance score. The best alternative has been chosen based on the ranking performance score (P_i), which will be quite nearer to the optimal measures. Table 6 displays the ranking produced by the TOPSIS approach for various WEDM machining conditions. From the table, it can be revealed that the order of performance score is 6–2-1–8-4–3-7–9-5.

3.3. *Desirability approach*

Desirability approach was introduced by Derringer and Suich in 1980.[28] It is one of the most widely used technique in manufacturing industries for optimizing the multi response problems. This technique can be employed to convert the multi response into a single response termed as composite desirability (d_G).[29] The given steps are to be taken by this approach,

Table 6. Performance score and their rank.

Ex. No.	S_i^+	S_i^-	P_i	Rank
1	0.068	0.067	0.4944	6
2	0.030	0.074	0.7087	2
3	0.030	0.085	0.7392	1
4	0.077	0.052	0.4048	8
5	0.045	0.062	0.5820	4
6	0.050	0.074	0.5984	3
7	0.076	0.065	0.4616	7
8	0.080	0.031	0.2803	9
9	0.058	0.063	0.5227	5

Step 1: Computing the individual desirability index (d_i) for the responses such as MRR and SR. Usually, three categories of objective followed according to the responses. Since we need higher MRR, then the objective function is selected as higher-the-better and the following equation is used.

$$d_i = \begin{cases} 1, & \hat{y} \le y_{\min} \\ \left(\dfrac{\hat{y}j - y_{\max}}{y_{\min} - y_{\max}}\right)^r, & y_{\min} \le \hat{y}j \le y_{\max}, \quad r \ge 0 \\ 0, & \hat{y} \ge y_{\max} \end{cases} \quad (11)$$

Similarly, we need lower SR, then the objective function is selected as lower-the-better and the following equation is used:

$$d_i = \begin{cases} 1, & \hat{y} \le y_{\min} \\ \left(\dfrac{\hat{y}j - y_{\min}}{y_{\min} - y_{\max}}\right)^r, & y_{\min} \le \hat{y}j \le y_{\max}, \quad r \ge 0 \\ 0, & \hat{y} \ge y_{\max} \end{cases} \quad (12)$$

where $y_{\max}$ & $y_{\min}$ – are the maximum and minimum value of "y".

Step 2: Determining the composite desirability (d_G) value by using Eqn. (13). The individual desirability index (d_i) of all the responses can be combined to form a single value called composite desirability (d_G)

$$d_G = \sqrt[w]{d1^{w1} * d2^{w2} * \cdots * di^{wi}}, \quad (13)$$

where d_i is the individual desirability index and w_i is the weight of response. Table 7 illustrates the value of composite desirability (d_G) and its rank.

The combined rank plot for performance score (P_i) and composite desirability (d_G) is shown in Fig. 2. From the plot, it can be understood that the experiment number 3 shows the highest value of P_i (0.7392) and d_G (0.7410), then the optimal combination of input parameters is I_p of 6 amps, T_{on} of 15 μs and T_{off} of 30 μs, which are producing higher MRR with lower SR for the fabricated composite.

Table 7. Composite desirability and its rank.

Ex. No.	Individual desirability (d_i) MRR	SR	Composite desirability (d_G)	Rank
1	0.1007	1.0000	0.3174	6
2	0.8126	0.5954	0.6955	2
3	1.0000	0.5491	0.7410	1
4	0.0043	0.7861	0.0582	7
5	0.7356	0.3988	0.5416	3
6	0.9449	0.2543	0.4902	4
7	0.0000	0.9769	0.0000	8
8	0.4105	0.0000	0.0000	9
9	0.8175	0.1561	0.3572	5

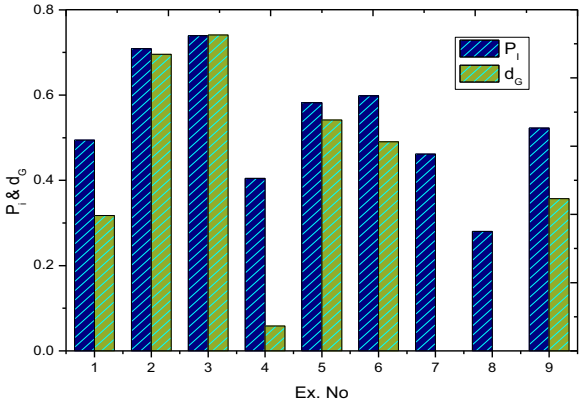

Fig. 2. Rank plot for P_i and d_G.

4. Results and Discussion

4.1. *Morphological analysis*

Figures 3(a) and 3(b) show the SEM micrograph and the EDS pattern for the proposed AZ31 Mg alloy composite reinforced with ZrO_2 and seashell powder. Figure 3(a) clearly shows the proper dispersion of ZrO_2 and seashell powder (SSP) in the matrix. The SEM image also indicates that the casting is free from voids due to proper casting parameters being utilized. The EDS spectrum of the sample is obtained at random region which ensures the presence of ZrO_2 and seashell powder in the form of calcium carbonate mixed with the matrix metal. The percentage composition obtained from the EDS as Mg in is 72.56 wt.%, C in 19.19 wt.%, O in 4.47 wt.%, respectively. The remaining elements Al, Zn, Zr and Ca are below 2 wt.%. The EDS image confirms the presence and percentage distribution of reinforcement mixes with the matrix alloy.

4.2. *Effect of machining parameters on MRR*

Figure 4 depicts the S/N ratio graph for MRR. From the graph, we noticed the effect of machining parameters on MRR. It clearly shows that MRR increases with low level of I_p (6 amps) and higher level of T_{on} (15 μs) and T_{off} (30 μs). During this condition, the longer spark duration generates plasma between the tool and work piece interface, then melting and evaporation occur on the work piece, thus enhance the MRR. Hence, the longer pulse duration and pulse current required removing the metal from the work specimen because of the inclusion of reinforcements producing hard surface that will resist easy metal removal.

Analyzing S/N ratio of the MRR in Taguchi qualitative tool "larger the better" is preferred. Table 8 depicts the S/N ratio response table for MRR. Generally, the influencing parameters are observed by higher delta value and ranked as 1. From response table, T_{on} plays a vital role in MRR having the delta value of 3.727 dB and is ranked as 1. It has been ascribed to increased thermal power with longer pulse-on time, which leads to a faster cutting rate. Pulse current (I_p) plays the next significant role in the MRR and delta value of 0.908 dB and is ranked as 2. Based on the results, T_{on} and I_p play a predominant role on MRR. This is due to longer spark duration developed between brass wire and work piece over the continuous current flow. Pulse-off time (T_{off}) plays the least role in MRR and the delta value of 0.317 dB and is ranked as 3.

ANOVA is a statistical approach which is employed to analyze the effect of independent input parameters on responses.[30,31] The precedence of the input parameters is considered based on F-value. From Table 9, it clearly noticed that the T_{on} and I_p play a significant role in machining of seashell and ZrO_2-reinforced AZ31 Mg alloy composite has an F-value of 60.16 and 3.94, respectively. Moreover, T_{off} influencing the MRR slightly lesser than other two process parameters gives an F-value of 0.65. T_{on} and I_p are the major factors representing the contribution of 91.49% and 5.99%, respectively. T_{off} less influencing factor with contribution of 0.97%. Similar results were concluded by Karthikeyan *et al.*[32] and they reported that T_{on} (84.13%) and I_p (14.58%) contribute more than T_{off} (0.29%) in the WEDM machining

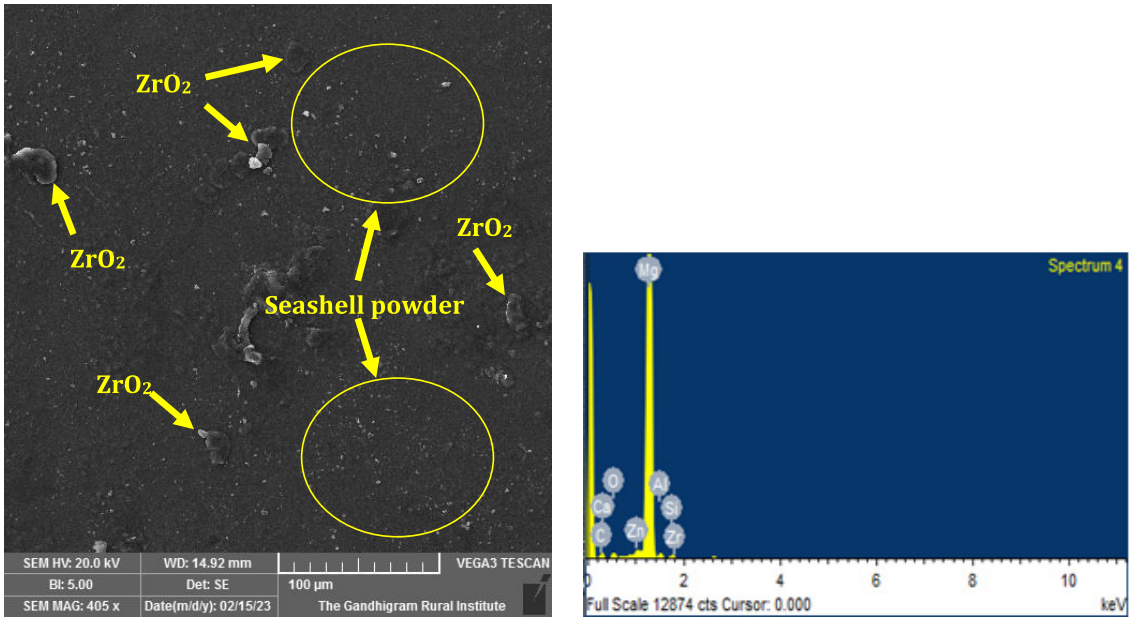

(a) (b)

Fig. 3. AZ31 Mg alloy-ZrO_2-Seashell composite (a) SEM image and (b) EDS image.

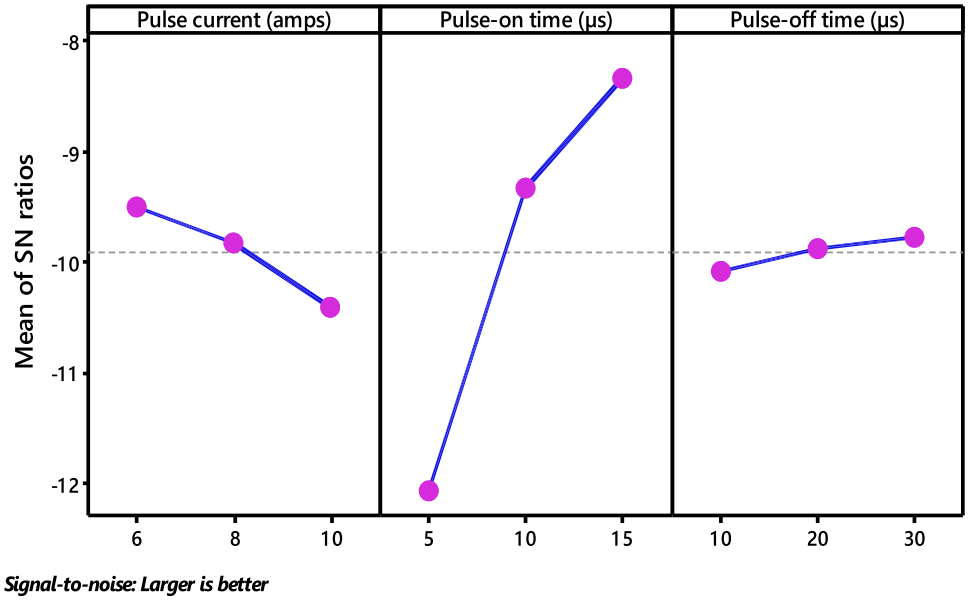

Fig. 4. S/N ratio plot for MRR.

of ZrO_2-reinforced aluminum matrix composite. R^2 and R^2(adj) values 98.48% 93.92% prove that the created model can successfully predict the MRR given the known input parameters.

The contour mapping of MRR is shown in Figs. 5(a)–5(c). From the graphs, we have understood the effect of machining parameters, namely I_p, T_{on} and T_{off} on the MRR during the WEDM process of the synthesized composite. Figure 5(a) reveals the interactive of I_p and T_{on} with MRR. It is clearly stated that the MRR progressively improved when T_{on} increases from 5 μs to 15 μs. Here, T_{on} is the

Table 8. S/N ratio table for MRR.

Level	I_p	T_{on}	T_{off}
1	−9.503	−12.068	−10.089
2	−9.826	−9.332	−9.880
3	−10.411	−8.340	−9.772
Delta	0.908	3.727	0.317
Rank	2	1	3

Table 9. ANOVA for MRR.

Source	DF	Seq. SS	Adj. MS	F-value	P(%)
I_p	2	0.0018474	0.0009237	3.94	5.99
T_{on}	2	0.0281861	0.0140930	60.16	91.49
T_{off}	2	0.0003038	0.0001519	0.65	0.986
Error	2	0.0004685	0.0002342	—	1.52
Total	8	0.0308057	—	—	—

$S = 0.0153052$; R-Sq = 98.48%; R-Sq(adj) = 93.92%

primary important factor for controlling the MRR. However, the MRR also depends on I_p, while considering higher I_p (10 amps), higher MRR (0.375 g/min) is obtained. Hence, the MRR has increased at all levels of I_p. At the initial level of T_{on} (5 μs), with all levels of I_p the lowest MRR (0.250–0.275 g/min) is produced. Similarly, the average MRR (0.300–0.325 g/min) has attained 7.5 μs of T_{on} with all levels of I_p. In Fig. 5(b), the effect of I_p and T_{off} with MRR is displayed. It has been noted that the MRR increases with an increase in I_p and T_{off}. Based on the plot, lower MRR (0.250 g/min) has attained 8 amps of I_p and 20 μs of T_{off}, respectively. Similarly, higher MRR (0.375 g/min) is produced at 6 amps of I_p with 30 μs of T_{off}. Thethe highest range of I_p (10 amps) with the middle range of T_{off} (20 μs) produce greater MRR with a range of 0.350–0.375 g/min, respectively. Meanwhile, 10 amps of I_p with 30 μs of T_{off} give the lesser MRR with a range of 0.250–0.275 g/min. The effect of T_{on} and T_{off} with MRR is depicted in Fig. 5(c). It was found that the larger MRR seems to have higher T_{on} (15 μs) with all levels of T_{off}. Here, the maximum MRR (0.375 g/min) is gained at 15 μs of T_{on} and 30 μs of T_{off}, respectively. In the mean time, the higher T_{off} with lower T_{on} produces less MRR (0.250 g/min). The moderate MRR is obtained at 10 μs of T_{on} with all levels of T_{off}.

4.3. *Effect of machining parameters on SR*

The S/N ratio graph for SR is illustrated in Fig. 6. The graph displays the effect of machining parameters on SR. It exactly reveals that SR decreases with low level of I_p (6 amps) and T_{on} (5 μs) and high

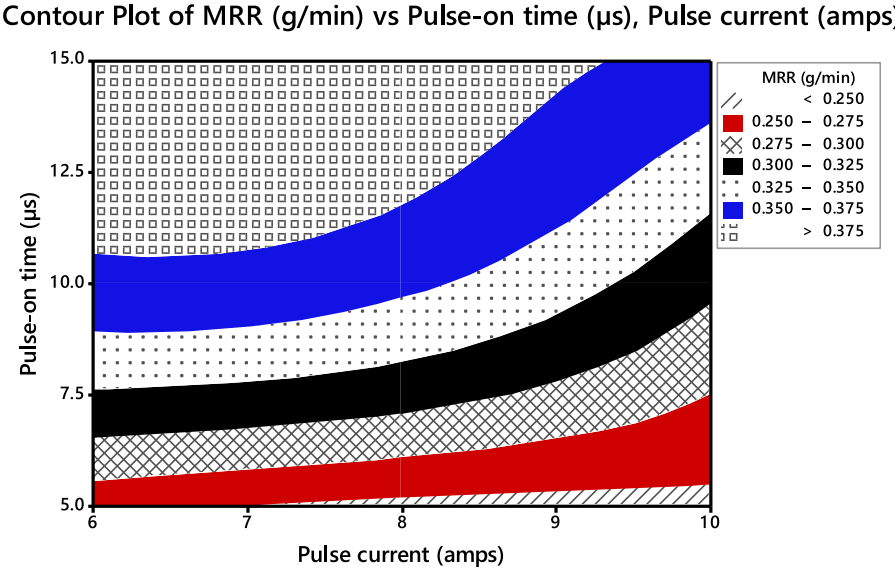

(a)

Fig. 5. Contour plot for MRR (a) I_p vs. T_{on}, (b) I_p vs. T_{on} and (c) T_{on} vs. T_{off}.

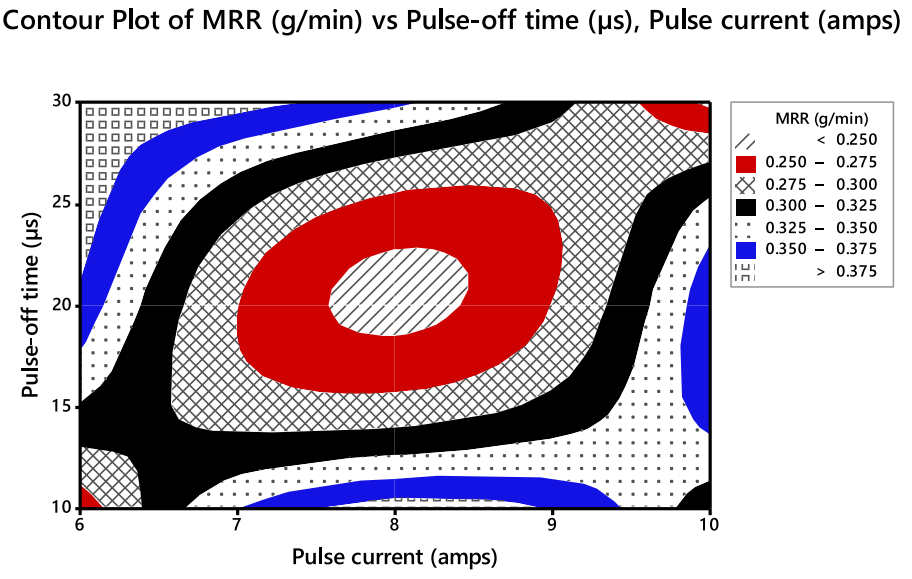

(b)

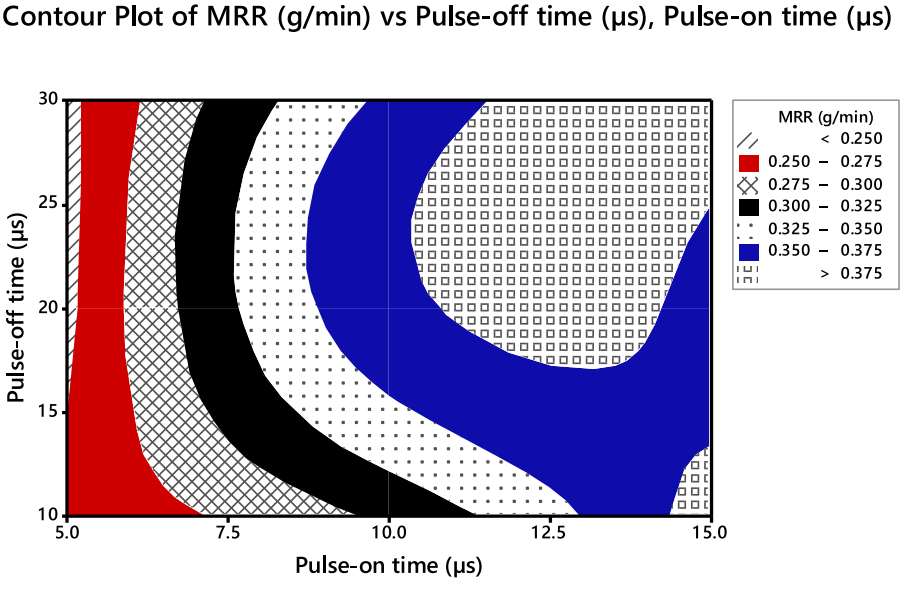

(c)

Fig. 5. (*Continued*)

level of T_{off} (30 μs), respectively. In this case, the SR steadily increases with an increase in pulse current. So that, the maximum SR obtained at a higher level of pulse current due to more power supplied at the machining region, thus creates craters and voids on the surface of the work piece. Moreover, the incorporation of reinforcement particles does not melt during machining, thus resulting in formation of rough surface. Similarly, the longer pulse duration produces more SR due to continuous spark between the tool and work piece.

The S/N ratio of the SR in Taguchi qualitative tool "smaller the better" is preferred. The response table for S/N ratio of SR is represented in Table 10. From response table, T_{on} shows a vigorous role in SR by a delta value of 2.19 dB and is ranked as 1. Pulse

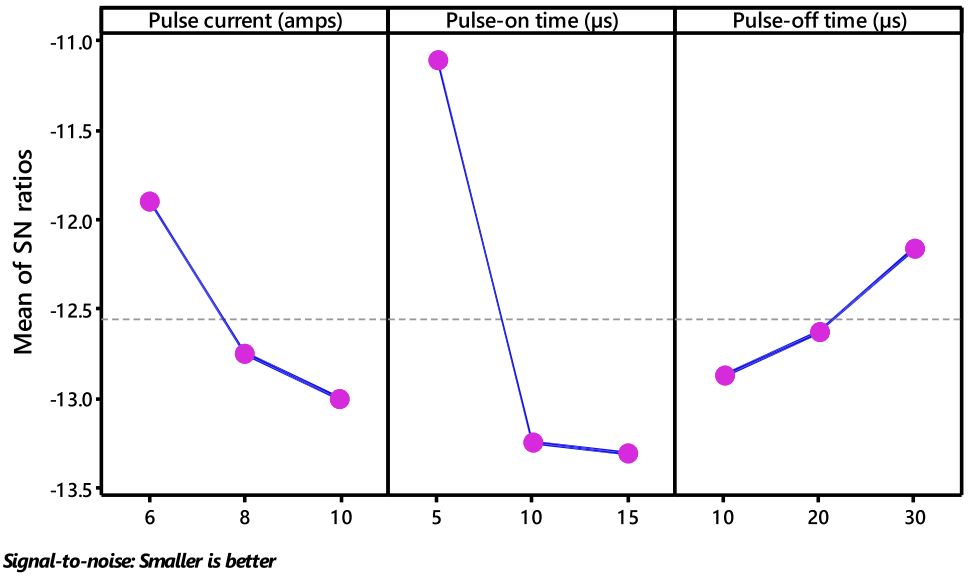

Fig. 6. S/N ratio plot for SR.

Table 10. S/N ratios for SR.

Level	I_p	T_{on}	T_{off}
1	−11.91	−11.12	−12.88
2	−12.76	−13.25	−12.63
3	−13.01	−13.31	−12.17
Delta	1.10	2.19	0.72
Rank	2	1	3

Table 11. ANOVA for SR.

Source	DF	Seq. SS	Adj. MS	F-value	P(%)
I_p	2	0.53687	0.26843	4.44	17.85
T_{on}	2	2.12240	1.06120	17.56	70.60
T_{off}	2	0.22607	0.11303	1.87	7.52
Error	2	0.12087	0.06043	—	4.02
Total	8	3.00620	—	—	—

$S = 0.245832$; R-Sq = 95.98%; R-Sq(adj) = 83.92%

current (I_p) plays next significant role in the SR and delta value of 1.10 dB and is ranked as 2. Pulse-off time (T_{off}) plays a least role in SR and the delta value of 0.72 dB and is ranked as 3. The increase in pulse current and pulse duration enhances the SR value due to more spark generated which creates craters over the surface of the machined composite. But, T_{off} has less significant factor which does not influence the SR during the machining process.

Table 11 depicts the results of ANOVA for SR. From the table, it is observed that the T_{on} which is the most noteworthy factor has an F-value of 17.56, followed by I_p with the F-value of 4.44, respectively. Moreover, T_{off} is an insignificant factor than the others with F-value of 1.87 only. T_{on} and I_p are the primary dominant factors with the contributions of 70.60% and 17.85%, respectively. T_{off} is less significant factor with contribution of 7.5%. Similar results were found by Rajendar Kumar *et al.*[33] during the WEDM process of ZE41A Mg alloy. R^2 and R^2(adj) values 95.98% and 83.92% expose that the model can predict the SR for input parameter effectually.

Figures 7(a)–7(c) demonstrate the contour mapping of SR with respect to WEDM parameters. The influence I_p and T_{on} with SR is seen in Fig. 7(a). It can be noticed that lower SR (3.6 μm) is given at initial level of I_p (6 amps) and T_{on} (5 μs). Furthermore, the SR increases gradually when I_p increased. The average SR value of 4.2–4.5 μm is obtained at 15 μs of T_{on} with all levels of I_p. Similarly, the maximum SR is produced at 10 amps of I_p with 12.5 μs of T_{on}. Figure 7(b) depicts the interaction of I_p and T_{off} with SR. It was noticed that the lowest SR of 3.6–3.9 μm is attained at 10 μs of T_{off} and 6 amps of I_p, respectively. Moreover, the SR significantly improved by increasing trends of I_p and T_{off}. Hence, an average SR value of 4.2–4.5 μm is produced at 30 μs of T_{off} with 8 amps of I_p. By considering 10 amps of I_p with 10 μs of T_{off} the SR value is enhanced to 5.1 μm. But, higher I_p (10 amps)

with 30 μs of T_{off} reduces the SR range of 3.6–3.9 μm, respectively. The interaction of T_{on} and T_{off} on SR is seen in Fig. 7(c). It was observed that the SR decreased with decrease in T_{on} and increase in T_{off}. Hence, lower SR is produced at lower levels of the T_{on} (5 μs) with high levels of T_{off} (30 μs). Although, a medium range of SR is obtained at 15 μs of T_{on} with T_{off} from 10 μs to 30 μs, respectively. Meanwhile, the maximum SR (4.8–5.1 μm) is attained at 15 μs of T_{on} with 20 μs of T_{off}. At the same time, the larger SR (5.1 μm) has been noticed at 10 μs of T_{on} with 10 μs of T_{off}, respectively.

4.4. *Effect of machining parameters on performance score (P_i)*

Figure 8 graphically depicts the mean plot for performance score (P_i) with respect to machining

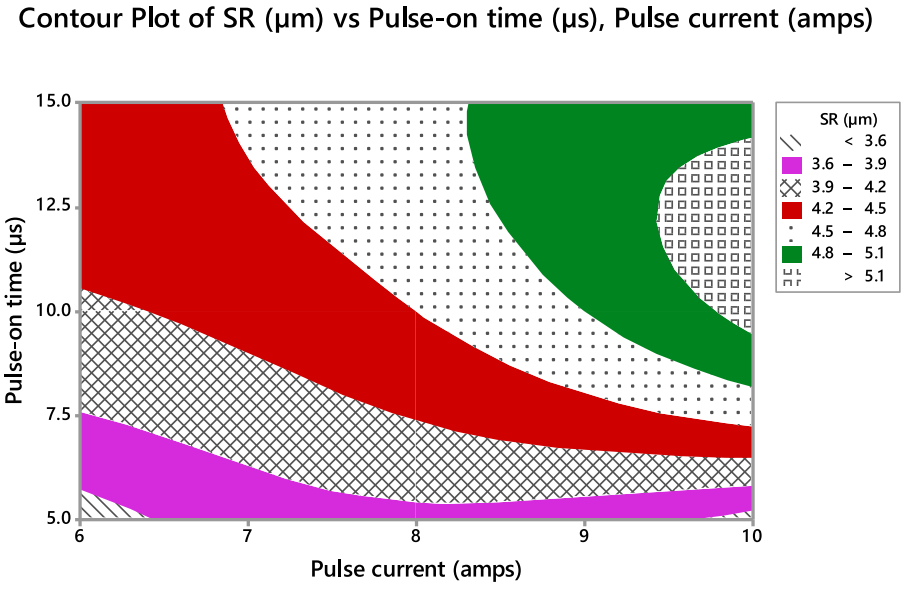

(a)

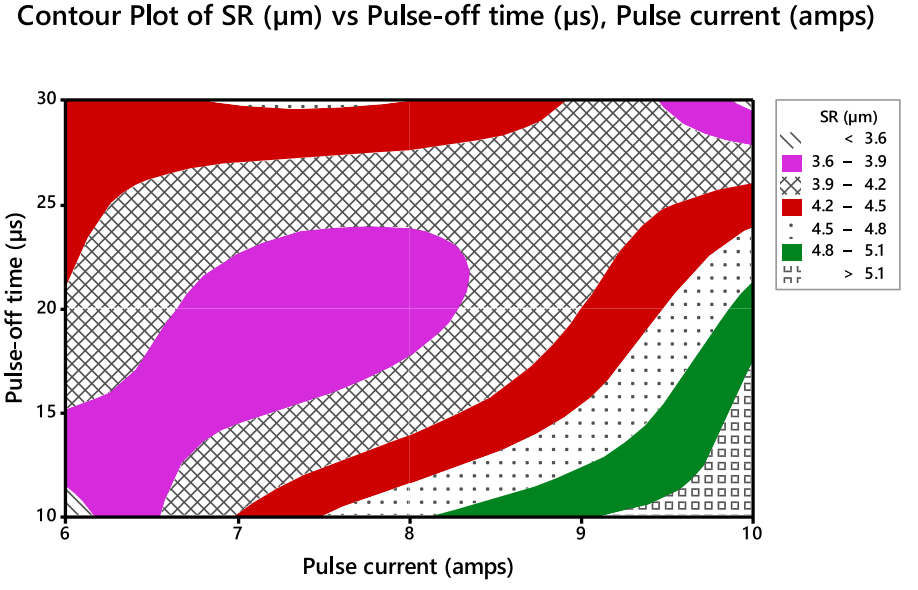

(b)

Fig. 7. Contour plot for SR (a) I_p vs. T_{on}, (b) I_p vs. T_{on} and (c) T_{on} vs. T_{off}.

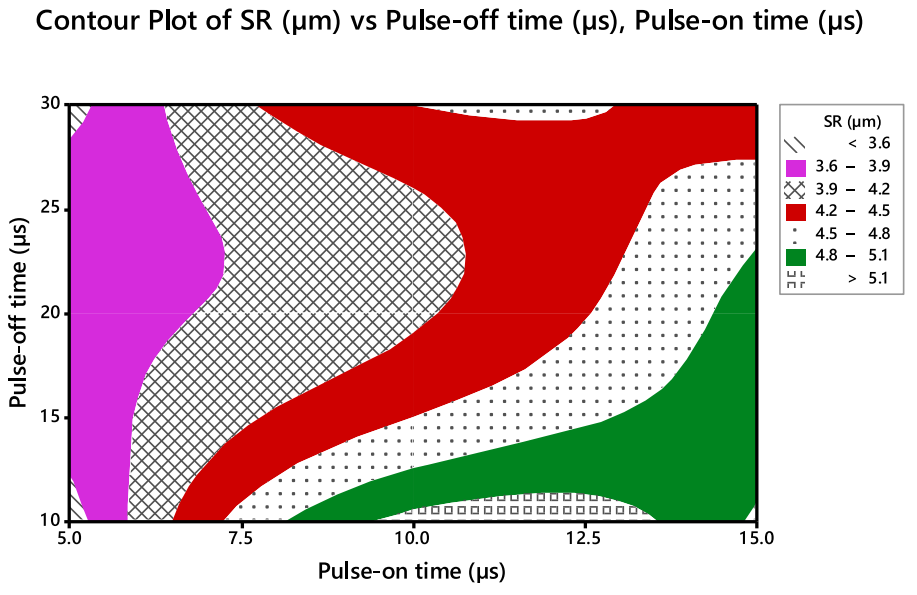

(c)

Fig. 7. (*Continued*)

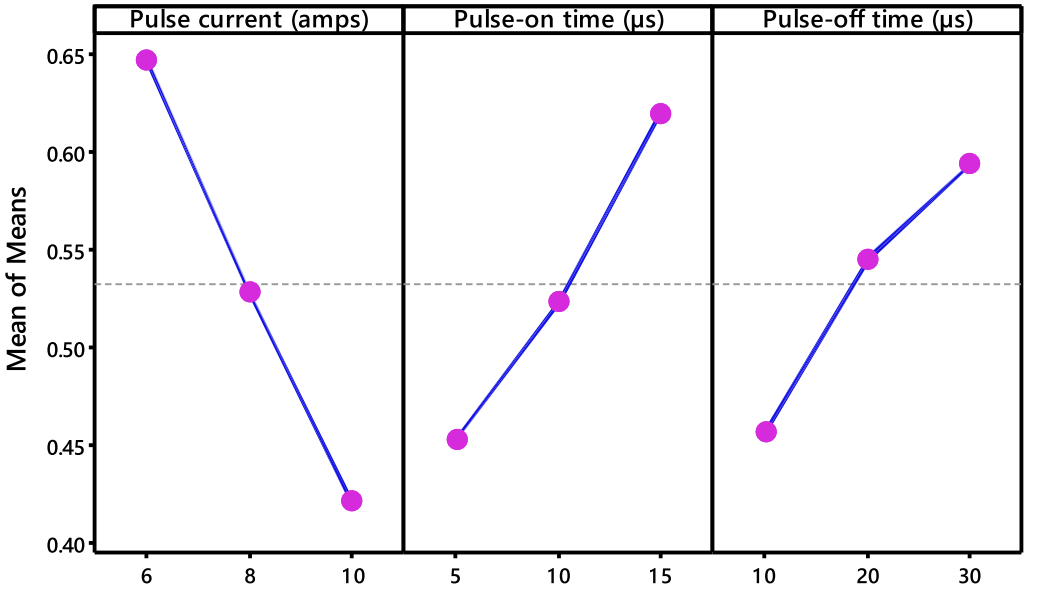

Fig. 8. Means plot for performance score (P_i).

parameters. From the graph, the optimal conditions of parameters for obtaining higher MRR with lower SR of the synthesized AZ31 Mg alloy composite reinforced with ZrO_2 and seashell powder are exactly seen. Based on the graph (Fig. 8), the optimal conditions of machining parameters are I_p at level 1 (6 amps), T_{on} at level 3 (15 μs) and T_{off} at level 3 (30 μs), respectively. It can be revealed that pulse current (I_p) has an important factor for MRR and SR. At the initial level of I_P high level of T_{on} produce more MRR and less SR. The reason is that the supply of spark energy is controlled by pulse duration. Hence, a longer pulse duration increases the MRR and decreases the SR due to continuous

Table 12. Means table for performance score (P_i).

Level	I_p	T_{on}	T_{off}
1	0.6474	0.4536	0.4577
2	0.5284	0.5237	0.5454
3	0.4215	0.6201	0.5943
Delta	0.2259	0.1665	0.1366
Rank	1	2	3

Table 13. ANOVA for performance score (P_i).

Source	DF	Seq. SS	Adj. MS	F-value	P(%)
I_p	2	0.076620	0.038310	3.88	45.86
T_{on}	2	0.041931	0.020965	2.12	25.10
T_{off}	2	0.028730	0.014365	1.45	17.19
Error	2	0.019770	0.009885	—	11.83
Total	8	0.167051	—	—	—
$S = 0.0994235$; R-Sq = 88.17%; R-Sq(adj) = 52.66%					

spark generated between the electrode and the work piece.

Table 12 shows the response table for mean performance score (P_i). From response table, pulse current (I_p) plays a predominant role in responses (MRR and SR) and the delta value of 0.2259 and is ranked as 1. After that, T_{on} is, the more significant factor, followed by T_{off} having the delta values of 0.1665 and 0.1366. This examination can be ensured by ANOVA. Table 13 presented the results of ANOVA for performance score. From the table, F-value of I_p (3.88) and T_{on} (2.12) is more than that of T_{off} (1.45), hence those are considered as more significant factors

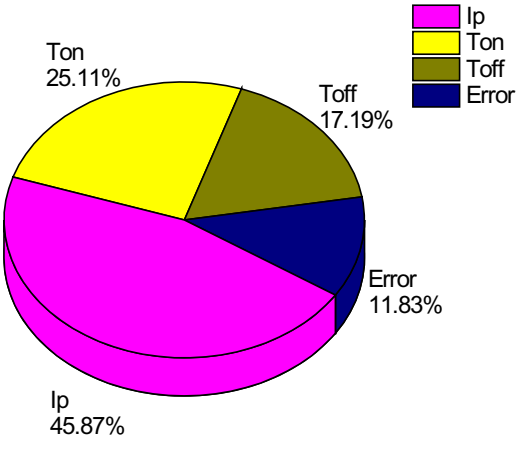

Fig. 9. Contribution of machining parameters on performance score (P_i).

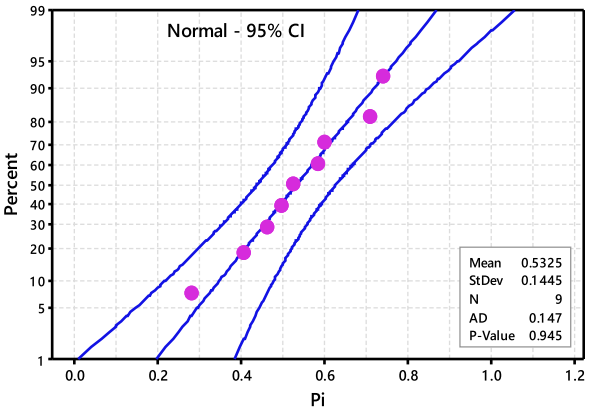

Fig. 10. Probability plot for performance score (P_i).

for influencing the MRR and SR during the WEDM process of developed composite. Figure 9 graphically represented the contribution of machining parameters on performance score. It has been found that the I_p was the preliminary noteworthy factor with a contribution of 45.86%, next by T_{on} and T_{off} having contributions of 25.10% and 17.19%, respectively. The similar observations were made by Alagarsamy *et al.*[34] while machining Al7075-TiO_2 composite. Figure 10 illustrates the probability graph for performance score and it confirms the existence of responses placed within the limits.

5. Conclusions

- In this work, AZ31 Mg alloy reinforced with ZrO_2 and seashell powder has been successfully fabricated through bottom pouring type stir casting method.
- SEM with EDS images confirms the presence of the reinforcements seashell powder and ZrO_2 is evenly distributed throughout the base alloy.
- The machinability behavior of the ZrO_2/seashell powder-reinforced AZ31 Mg alloy composite was analyzed in WEDM facility. The optimal conditions of parameter in WEDM such as pulse current (I_p), pulse-on time (T_{on}) and pulse-off time (T_{off}) for attaining maximum MRR and minimum SR were found by using Taguchi coupled TOPSIS and desirability approach.
- From Taguchi results, it has been observed that the MRR increases at the parameter combination of 6 amps I_p, 15 μs T_{on} and 30 μs T_{off}. Similarly, SR

decreases at 6 amps I_p, 5 μs T_{on} and 30 μs T_{off}, respectively.

- From TOPSIS results, it has been identified that the experiment number 3 has attained higher performance score (0.7392) then the corresponding level of machining parameters is closer to the optimal conditions. From means graph, it can be revealed that the maximum MRR with minimum SR is produced at 6 amps of I_p, 15 μs of T_{on} and 30 μs of T_{off}.
- ANOVA results confirmed that the order of significant parameters affects the MRR and SR and I_p, T_{on}, and T_{off} have contributions of 45.86%, 25.60% and 17.19%, respectively.

References

1. M. P. Staiger, A. M. Pietak, J. Huadmai and G. Dias, *Biomaterials* **27** (2006) 1728–1734.
2. H. M. Wong, K. W. K. Yeung *et al.*, *Biomaterials* **31** (2010) 2084–2096.
3. Z. S. S. Najeeb and Z. Khurshid, *Materials* **8** (2015) 5744–5794.
4. F. Witte, V. Kaese and H. Haferkamp, *Biomaterials* **26** (2005) 3557–3563.
5. K. W. K. Yeung and K. H. M. Wong, *Technol. Health. Care* **20** (2012) 345–362.
6. H. Khakbaz, R. Walter, T. Gordon and M. B. Kannan, *Mater. Res. Express* **1** (2014) 045406.
7. M. Sheth, N. Sheth and N. Radadia, *Mater. Res. Express* **6** (2019) 1–10.
8. M. A. Razak, A. M. Abdul-Rani and T. V. V. L. N. Rao, *Procedia. Eng.* **148** (2016) 916–922.
9. S. Vijayabhaskar and T. Rajmohan, *Silicon* **11** (2019) 1701–1716.
10. R. S. Gill, K. Kumar and U. Batra, *J. Mater. Eng. Perform* **30** (2021) 2955–2966.
11. R. Karthik, R. Viswanathan, J. Balaji, N. Sivashankar and R. Arivazhagan, *IOP Conf. Series: Mater. Sci. Eng* **1013** (2021) 1–9.
12. A. Muniappan, M. Sriram, C. Thiagarajan, G. B. Raja and T. Shaafi, *IOP Conf. Ser., Mater. Sci. Eng.* **390** (2018) 1–6.
13. V. Kavimani, K. S. Prakash and T. Thankachan, *Measurement* **145** (2019) 335–349.
14. V. Bhuvaneswari, L. Rajeshkumar, R. Saravanakumar and D. Balaji, *Arch. Metall. Mater.* **67** (2021) 1217–1226.
15. D. Dash, S. Samanta and R. N. Rai, *IOP Conf. Ser., Mater. Sci. Eng.* **377** (2018) 012133.
16. K. Manikandan, P. Ranjith Kumar, D. Raj Kumar and K. Palanikumar, *J. Mater. Res. Technol.* **9** (2020) 12260–12272.
17. V. K. Saini, Z. A. Khan and A. N. Siddiquee, *Int. J. Mech. Prod. Eng.* **2** (2013) 61–64.
18. S. V. Alagarsamy, R. Balasundaram, M. Ravichandran *et al.*, *Surf. Topogr. Metrol. Prop.* **9** (2021) 1–15.
19. A. Ikram, N. A. Mufti, M. Q. Saleem and A. R. Khan, *J. Mech. Sci. Technol.* **27** (2013) 2133–2141.
20. P. Raveendran, S. V. Alagarsamy, C. Chanakyan *et al.*, *Surf. Topogr: Metrol. Prop.* **9** (2021) 1–12.
21. S. V. Alagarsamy, P. Raveendran and M. Ravichandran, *Silicon* **13** (2020) 2529–2543.
22. A. K. Parida and B. C. Routara, *Int. Sch. Res. Notices* **905828** (2014) 1–10.
23. P. H. Nguyen, T. Muthuramalingam, D. V. Pham, S. Shirguppikar *et al.*, *Sadhana* **47** (2022) 1–12.
24. V. R. Vaddi, C. S. Reddy, S. K. Bushaboina and H. Banka, *SAE Tech. Paper* (2018) 1–7.
25. S. K. Sahoo, S. S. Naik and J. Rana, *Int. J. Process. Manag. Benchmarking* **9** (2019) 216–231.
26. M. Kalayarasan and M. Murali, *Int. J. Eng. Res. Africa* **22** (2016) 83–93.
27. G. Kaur and M. K. Gaur, *J. Ind. Saf. Eng.* **3** (2016) 1–8.
28. S. K. Sahoo, S. S. Naik and J. Rana, *Int. J. Process. Manag. Benchmarking* **9** (2019) 216–231.
29. S. V. Alagarsamy, M. Ravichandran and H. Saravanan, *J. Adv. Manuf. Syst.* **20** (2021) 1–26.
30. A. Majumder, P. K. Das, A. Majumder and M. Debnath, *Prod. Manuf. Res.* **2** (2014) 228–240.
31. M. Meignanamoorthy, M. Ravichandran, S. Sakthivelu *et al.*, *Mater. Today, Proc.* **27** (2020) 1051–1054.
32. K. Karthikeyan, S. V. Alagarsamy and C. Ilaiyaperumal, *Surf. Rev. Lett.* **29** (2021) 1–11.
33. R. Kumar, P. Katyal and S. Mandhania, *Int. J. Lightweight Mater. Manuf.* **5** (2022) 543–554.
34. S. V. Alagarsamy, M. Ravichandran, S. D. Kumar, S. Sakthivelu, M. Meignanamoorthy and C. Chanakyan, *Mater. Today, Proc.* **27** (2020) 853–858.